Cell PRESS

Structure
Article

Capsomer Dynamics and Stabilization in the T = 12 Marine Bacteriophage SIO-2 and Its Procapsid Studied by CryoEM

Gabriel C. Lander,[1,2,4] Anne-Claire Baudoux,[3,5] Farooq Azam,[3] Clinton S. Potter,[1] Bridget Carragher,[1] and John E. Johnson[2,*]
[1]National Resource for Automated Molecular Microscopy
[2]Department of Molecular Biology
The Scripps Research Institute, La Jolla, CA 92037, USA
[3]Scripps Institution of Oceanography, Marine Biology Research Division, University of California, San Diego, La Jolla, CA 92037, USA
[4]Present address: Life Science Division, Lawrence Berkeley National Lab, 1 Cyclotron Road, Berkeley, CA 94720, USA
[5]Present address: Institut Universitaire Européen de la Mer, Laboratoire des Sciences de l'Environnement Marin, 29280 Plouzané, France
*Correspondence: jackj@scripps.edu
DOI 10.1016/j.str.2012.01.007

SUMMARY

We report the subnanometer cryo-electron microscopy (cryoEM) reconstruction of a marine siphovirus, the Vibrio phage SIO-2. This phage is lytic for related Vibrio species with significant ecological importance, including the broadly antagonistic bacterium *Vibrio sp*. SWAT3. The three-dimensional structure of the 800 Å SIO-2, icosahedrally averaged head of the tailed particle revealed a T = 12 quasi-symmetry not previously described in a bacteriophage. Two morphologically distinct types of auxiliary proteins were also identified; one species bound to the surface of hexamers, and the other bound to pentamers. The secondary structure, evident in the electron density, shows that the major capsid protein has the HK97-like fold. The three-dimensional structure of the procapsid form, also presented here, has no "decoration" proteins and reveals a capsomer organization due to the constraints of the T = 12 symmetry.

INTRODUCTION

A variety of data indicate that dsDNA bacteriophages are the most abundant biomaterial on earth (Hendrix, 2002; Suttle, 2007). It is estimated that a mole of these bacteriophages infect their hosts every second. What's more, a common ancestor was infecting hosts before the separation of the three domains of life more than 3 billion years ago (Bamford et al., 2005; Hendrix, 1999). As a replicating entity, these viruses have had ample opportunity to explore virtually every niche of evolutionary space and have converged on a general assembly and maturation strategy that is recognizable in all dsDNA bacteriophages that have been investigated to date as well as in the animal herpesviruses (Baker et al., 2005; Duda et al., 2006; Johnson, 2010). Superimposed on the general principles are a variety of nuances that flavor the study of bacteriophages with interesting tangents readily discerned by structural studies (Wikoff et al., 2000). To our knowledge, among the more novel bacteriophages recently investigated is the Scripps Institute of Oceanography-isolate 2 (SIO-2) that infects the marine bacteria *Vibrionales Vibrio* sp. SWAT-3. It was shown that the SIO-2 host plays a significant role in structuring the bacterioplankton community, with far-reaching ecological implications (Long and Azam, 2001).

SIO-2 is a siphovirus with an 80,000 base genome, packaged in an 800 Å particle. Here, we report the subnanometer structure of the SIO-2 mature particle and show that it contains, to our knowledge, a novel T = 12 quasi-equivalent surface lattice. In addition to the major capsid protein, there are two additional prominent gene products in the capsid, one bound to the hexamer capsomers and the other bound to the pentamers. SIO-2 undergoes maturation, as do all other dsDNA bacteriophages investigated, and we also determined the 15 Å resolution structure of the round, 600 Å procapsid. Maturation creates the binding sites for the auxiliary proteins that are only present in the faceted mature particle. The quasi-symmetry of SIO-2 has not been previously seen in bacteriophages, and the positioning of capsomers required for this surface lattice places quasi-hexamers on icosahedral twofold and threefold axes, constraining these capsomers in the mature and procapsid in a manner not previously observed.

RESULTS

Purified SIO-2 phage were isolated from a host culture and examined with transmission electron microscopy (EM) under frozen hydrated conditions (Figure 1). SIO-2 particles exhibited thin angular capsid shells packed with double-stranded DNA (dsDNA). Bi-lobed decoration proteins were seen projecting from the smooth capsid surface in the raw images. The SIO-2 phage tail is 2090 Å in length, flexible, and occupies a fivefold vertex of the particle. SIO-2 capsid particle densities were extracted from the raw images and a three-dimensional (3D) reconstruction was computed. Icosahedral symmetry was applied during the reconstruction (the tails were averaged with other fivefold vertices and are not visible in the reconstructions) in order to maximize the signal in the raw images, resulting in electron density resolvable to subnanometer resolution (Figures 2

 ©2012 Elsevier Ltd All rights reserved

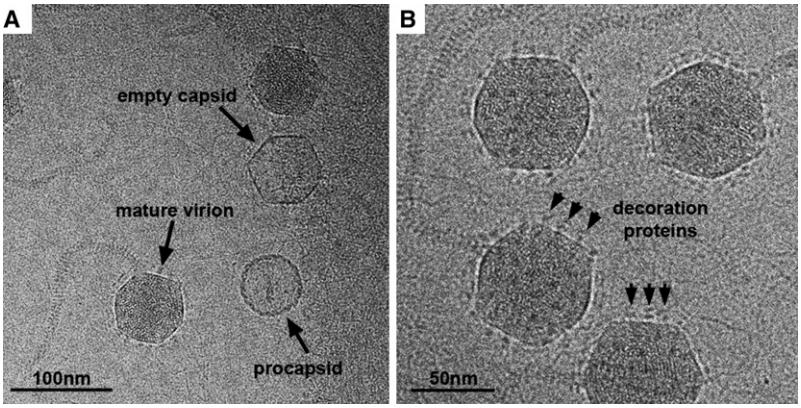

Figure 1. Images of SIO-2 Embedded in Vitreous Ice

(A) A full 4K × 4K micrograph in which a prohead particle, a mature virion, and an empty capsid shell are visible.

(B) A close-up view of mature virion particles, in which the double-layered decoration proteins can be observed (black arrows).

and 3). The capsid protein resolution was calculated by the Fourier shell correlation at 0.5 as 8.5 Å (Harauz and Van Heel, 1986; Sousa and Grigorieff, 2007). This statistics-based resolution estimate suffers due to disordered dsDNA within the capsid. The ordered protein details are consistent with electron density at subnanometer resolution, with clearly visible secondary structural elements (Figure 3).

The 800 Å capsid shell exhibits T = 12 quasi-symmetry (Figure 2) (Caspar and Klug, 1962) with two, structurally distinct, classes of decoration proteins—one class that binds specifically to the pentamer subunits and the other class localizing to the center of the hexameric capsomers. The quality of the reconstructed electron density enables clear delineation of the boundaries between the decoration protein and the capsid shell, as well as intersubunit boundaries within the icosahedral subunit. A genomic analysis of SIO-2 performed in parallel (Baudoux et al., 2012) was unable to make gene assignments for the decoration proteins but characterized the major capsid protein to be the product of gene 84, corresponding to a 29 kD band on an SDS-PAGE gel of purified particles. The segmented subunit density agrees well with the fold observed in HK97 (Helgstrand et al., 2003) and many other bacteriophages (Agirrezabala et al., 2007; Baker et al., 2005; Fokine et al., 2005; Jiang et al., 2008, 2006; Morais et al., 2005; Wikoff et al., 2000), displaying an overall triangular shape with a 40-Å-long helix traversing much of the subunit.

The two classes of decoration proteins bind to either 5-fold or quasi-6-fold capsomers. They are specific in their geometric selection (Figure 4) and strikingly different in their appearance and mode of interaction with capsid subunits. The hexamer-binding decoration proteins attach to the very central portion of the capsomer, and the observed electron density is consistent with interactions that take place via extended helices that insert into the hexamer central cavity. The capsomer interaction portion of this decoration protein is 6-fold symmetric, while the rest of the protein is not. The helical densities of the decoration protein converge to a bundle about 20 Å above the capsid surface and then blossom into two sequential mushroom-shaped clouds (~65 Å in diameter) roughly 40 and 80 Å above the hexamer surface (Figure 2). While these characteristic mushroom-like features are clearly visible in raw images (Figure 1), their reconstructed densities were not resolvable to the same degree as the capsid density, indicating that these densities either do not adhere to the icosahedral symmetry or are somewhat flexible.

The five pentamer-binding decoration proteins located at 11 of the 12 icosahedral vertices (the tail occupies the 12th) were readily segmented from the averaged density and have secondary structure features consistent with an immunoglobulin-like (Ig-like) fold (Figure 5). These proteins interact with individual pentamer subunits without invading the central pentamer cavity or mediating interactions between pentamer subunits. Effectively, they add an Ig-like domain to the pentamer subunits with no indication of adding stability to the capsid.

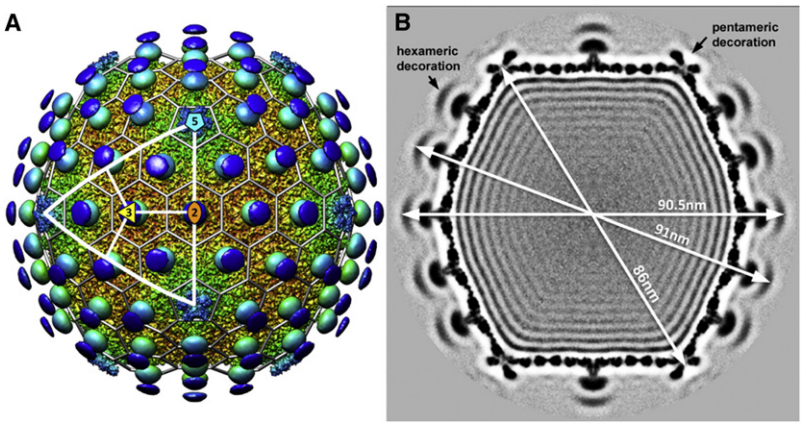

Figure 2. Icosahedral Reconstruction of the SIO-2 Capsid at Subnanometer Resolution

(A) An isosurface representation of the SIO-2 virion viewed down the twofold axis (VIPER orientation) at a sigma level of 1.5. The surface is colored radially from the center (red) of the capsid to the exterior (blue). The density corresponding to the disordered hexameric decoration proteins were computationally segmented and low-pass filtered so that their overall shape and dimension could be observed in the context of the higher resolution capsid surface. One icosahedral face of the capsid is outlined by a triangle, with the fivefold, threefold, and twofold axes labeled with a blue pentamer, yellow triangle, and orange oval, respectively.

(B) Central section through the virion reconstruction using a grayscale representation in which the weakest density is white and the strongest is black. The virus dimensions across the twofold, threefold, and fivefold axes are 90.5, 91, and 86 nm, respectively. Densities corresponding to the pentameric and hexameric decoration proteins are marked, and the disordered nature of the double-layered hexameric protein can be observed.

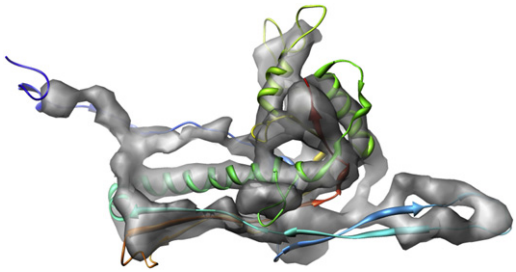

Figure 3. One Asymmetric Unit of the Mature SIO-2 Capsid
Density corresponding to a single asymmetric unit of the SIO-2 is shown as a transparent isosurface, with a ribbon representation of the HK97 gp5 (PDB ID: 1OHG) superimposed.

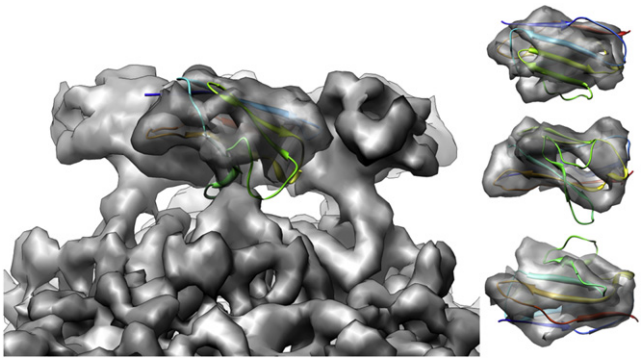

Figure 5. The Pentameric Decoration Protein Contains an Ig-like Fold
The crystal structure of an antibody Ig domain (PDB ID: 1a2y) was docked into the extracted density corresponding to a single monomer of the pentameric decoration protein.

The cryo-electron microscopy (cryoEM) micrographs also exhibited a small percentage of particles that were small and spherical, with thick shells and lacking tails. These characteristics are consistent with prohead particles—immature SIO-2 phage that have not undergone genome packaging and capsid expansion. The prohead particles lacked decoration proteins when viewed in the raw micrographs or reconstructed density. The prohead particles were boxed, and a 3D reconstruction was computed. Due to the small number of particles contributing to the reconstruction, the resolution was 15 Å, but the capsid subunits making up the pentameric and hexameric capsomers was clearly delineated. Hexamers are skewed (forming dimers of trimers) in the SIO-2 prophage, with the exception of the capsomers situated on the icosahedral threefold axes. This prophage hexamer is symmetric due to the symmetry constraint imposed by the threefold icosahedral symmetry. A dramatic rearrangement of the capsid proteins accompanies SIO-2 maturation as the subunit dispositions are strikingly different in the procapsid and capsid.

DISCUSSION

SIO-2 is the first example, to our knowledge, of a bacteriophage exhibiting a T = 12 surface lattice. This rare viral symmetry was observed in lower resolution studies of two viruses belonging to the *Bunyaviridae* family: Uukuniemi virus and Rift Valley fever virus, which arrange glycoproteins into an icosahedral lattice surrounding a lipid bilayer. (Freiberg et al., 2008; Huiskonen et al., 2009; Overby et al., 2008). While Uukuniemi virion capsids display variable morphologies that include T = 12 quasi-symmetry, Rift Valley fever virus particles exhibit icosahedral symmetry with a capsomer distribution consistent with this surface lattice. T = 12 quasi-symmetry requires hexameric capsomers to occupy threefold and twofold icosahedral symmetry positions. A theory referred to as "hexameric complexity" (Mannige and Brooks, 2010) posits that, as the size of the capsid shell increases, the geometric constraints imposed by the pentameric vertices on the organization of the hexamers become more complex. T = 12 symmetry is unfavorable, according to this theory, due to the large variety of intersubunit geometries necessary to achieve this quasi-symmetry. While a direct comparison of the dihedral angles between the SIO-2 capsid subunits is complicated by the elaborate and entangled protein interactions,

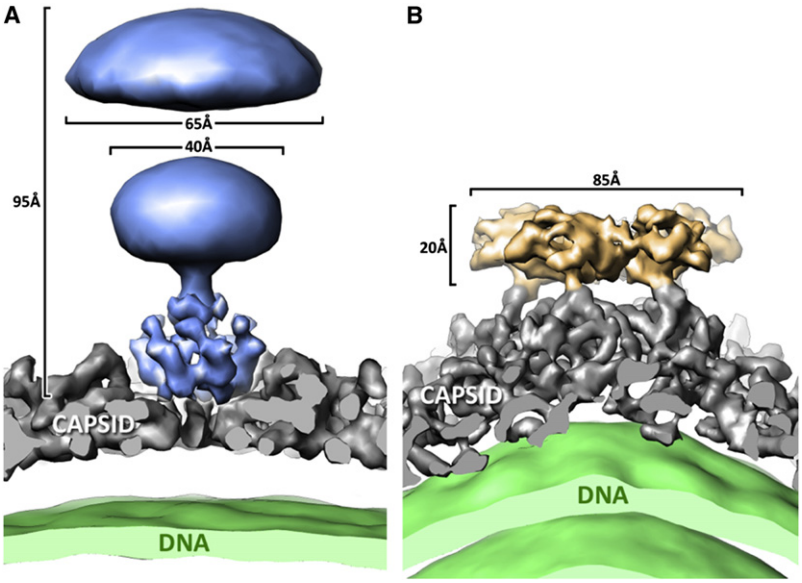

Figure 4. The Two Families of SIO-2 Decoration Proteins
(A) Side view of an isosurface representation of the hexameric decoration protein (blue) as it is seated at the center of a capsomer. As in Figure 2A, the two disordered mushroom-shaped densities were low-pass filtered to depict their overall shape and size. Capsid density is shown in gray, with DNA in green.
(B) Side view of an isosurface representation of the pentameric decoration protein (orange).

 ©2012 Elsevier Ltd All rights reserved

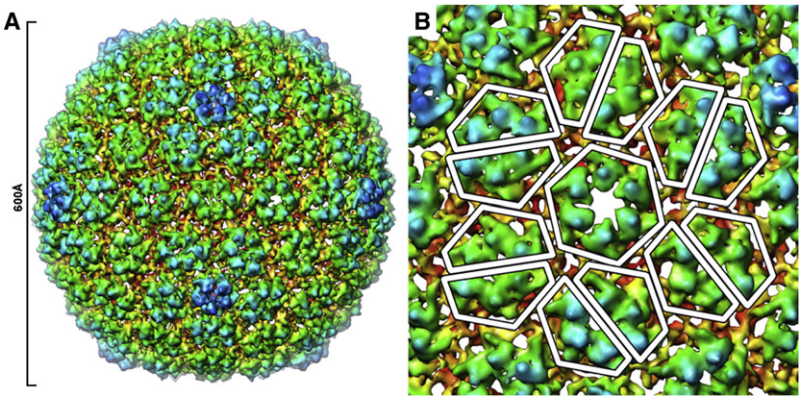

Figure 6. Icosahedral Reconstruction of the SIO-2 Prohead

(A) An isosurface representation of the SIO-2 prohead in the same orientation and using the same color scheme as Figure 2A.

(B) Close-up view of the icosahedral threefold axis, depicting a sixfold symmetric capsomer surrounded by six skewed hexameric capsomers.

as well as only moderate resolution, the particle does reflect an exceptional assortment of capsomer interactions. The capsid strain predicted by the geometric theory, however, is not reflected in the particle strength, as results from stability assays (Baudoux et al., 2012) show that SIO-2 is tolerant of a wide range of chemical, physical, and environmental factors.

Aside from its unusual T number, a striking feature of SIO-2 is the occurrence of two species of decoration proteins protruding from the capsid surface. While some capsids with T = 7 symmetry, such as bacteriophage lambda, have auxiliary capsid proteins (Lander et al., 2008), experimental observation indicates that all assemblies with a T number greater than 7 involve the attachment of stabilizing auxiliary proteins to complete maturation. SIO-2 incorporates two different proteins on its capsid shell, one that likely strengthens hexamers and one that adds an external domain to pentamers without contributing to their stability. Based on the similarity of the extracted SIO-2 asymmetric subunit to the HK97 crystal structure, it is clear that there are no additional proteins binding between the capsomers, nor has the subunit added a stabilization domain into its tertiary structure as in the P22 subunit through evolution (Parent et al., 2010). Thus, intercapsomer contacts are not strengthened beyond typical protein-protein interactions, making it plausible that, to our knowledge, this novel quasi-symmetric geometry shifts the stabilization requirements such that the hexamer centers, rather than intercapsomer interactions, must be fortified as observed in phage lambda.

SIO-2 procapsids have one hexameric capsomer per asymmetric unit located on an icosahedral threefold symmetry axis, and, unlike the other hexamers that are skewed in pseudo-twofold related trapezoids in the procapsid, this hexamer maintains sixfold symmetry from assembly of the procapsid to maturation. In contrast, the hexamer capsomers on the icosahedral twofold axes show the dimer of trapezoids, as do the hexamers that are unconstrained by particle symmetry (Figure 6). While skewed procapsid hexamers are frequently referred to as "a dimer of trimers," this is the first example of twofold icosahedral symmetry being imposed on the skewed hexamer, thereby confirming the terminology. Gertsman et al. postulate that skewing of hexamers is induced by capsomer interactions with the scaffold protein prior to assembly (Gertsman et al., 2009). Skewing in HK97 procapsids induces tertiary structure strain that is balanced by the interaction with the subunit scaffold domain prior to assembly. Following assembly, the scaffold domain is released, and the high-energy, strained, tertiary structure is maintained by quaternary interactions in the particle. The strained tertiary structure provides stored energy to make the HK97 procapsid metastable, providing an exothermic energy landscape to drive the quaternary structure changes associated with maturation (Johnson, 2010). If we assume the same scenario for SIO-2, then two of the three hexamers in the procapsid would have strained tertiary structures as in HK97; the hexamer on the threefold axis would, however, have the tertiary structure more like the mature particle. This implies an interesting capsomer dynamic during assembly where the constraints of icosahedral symmetry trump the distortion induced by the scaffolding protein with the possible release of the scaffold protein, loss of distortion in the subunit tertiary structure, and symmetrization of this hexamer. The SIO-2 procapsid is not of sufficient resolution to assert that it is identical to the fully mature hexamer. Again, referring to HK97, the hexamers in the first expansion intermediate are clearly symmetric, but they undergo significant further changes in quaternary organization as the particles proceed down the maturation pathway (Gan et al., 2006; Lee et al., 2005). Thus, the SIO-2 procapsid hexamer with threefold imposed symmetry may assume a similar intermediate conformation between skewed hexamers and fully mature hexamers.

The pentameric capsomers, which do not contain a central pore that is as large as those observed in the hexameric capsomers, always maintain strict fivefold symmetry. These vertices are likely to have more rigid intersubunit interactions, as their assembly does not require malleable surface associations like the hexamers. As such, structural strengthening at these vertices is unnecessary, yet the pentamer subunits serve as binding sites for decoration proteins. The fivefold symmetric density attached to the pentameric vertices exhibit a beta-sandwich envelope, consistent with an Ig-like domain fold. There are many examples of Ig-like domains in dsDNA phage structural proteins, and although their precise role in the phage life cycle remains uncertain, these domains likely aid in recognition and attachment to the host (Fokine et al., 2011). While no Ig-like domains are observed in single-stranded DNA or RNA phages, analysis of known dsDNA phage genomes show that approximately 25% encode for at least one Ig-like domain (Fraser et al., 2006). We hypothesize that, while the mushroom-like proteins binding at sites of local sixfold symmetry aid in stabilizing the capsid architecture, the Ig-like domains attached to the pentameric subunits may participate in cell recognition through a generalized attraction that precedes the tail interaction associated with DNA delivery into the cell.

The SIO-2 phage is a model of evolution's structural workaround, resulting in a stable infectious virion with an unlikely geometry. Further investigation of this virus protein lattice will strengthen our knowledge of protein physics in the context of large macromolecular assemblies. The role that the decoration proteins play in the SIO-2 life cycle will be examined in more detail to determine if the cited hypotheses have merit. A more detailed prophage structure would provide mechanistic understanding of quaternary structure dynamics under symmetry-constrained circumstances.

EXPERIMENTAL PROCEDURES

Phage Isolation and Purification

SIO-2 bacteriophage suspensions (180 ml) were recovered from plaque assays, as described elsewhere (Baudoux et al., 2012). Large cell debris were removed by low-speed centrifugation (10,000 × g, 30 min at 8°C). followed by filtration through polycobonate filters (0.2 μm, Nuclepore). Phages were pelleted by ultracentrifugation (141,000 × g, 2 hr at 8°C) and resuspended in 100 μl of 100-kDa-filtered autoclaved seawater (FASW). Phages were purified through a linear sucrose gradient (10%–40% in FASW) centrifugation (40,000 × g, 1 hr at 8°C), and the phage band was extracted with a sterile syringe. The purified phage were diluted in FASW and pelleted by ultracentrifugation to remove the sucrose and concentrate the sample (141,000 × g, 2 hr at 8°C). The pellet was gently resuspended in 50 μl of FASW and stored at 4°C until EM analysis.

CryoEM

Purified SIO-2 phage particles were prepared for cryoEM analysis by preservation in vitreous ice. C-flat (Protochips, Inc.) carbon-coated grids were glow-discharged in a Solarus (Gatan, Inc.) plasma cleaner for 6 s (75% argon, 25% oxygen), on to which 3 μl aliquots of sample were placed. The grids were transferred to a Vitrobot (FEI Co.) that was set to maintain a temperature of 4°C and 100% humidity, with an offset of −2 mm. Grids were blotted for 4 s, immediately plunged into liquid ethane, and subsequently transferred to liquid nitrogen and stored until they were loaded into the electron microscope.

Data were acquired on a Tecnai F20 Twin transmission electron microscope operating at 200 keV, using a dose of ~30 e-/Å^2 and a nominal underfocus ranging from 1.8 to 3.0 μm. Two data sets containing 3,554 and 3,074 images were automatically collected using a nominal magnification of 80,000× at a pixel size of 0.975 Å at the specimen level. We recorded all images with a Tietz F415 4K × 4K pixel CCD camera (15 μm pixel) utilizing the Leginon data collection software (Suloway et al., 2005).

Data Processing

Experimental data were processed by the Appion software package (Lander et al., 2009), which interfaces with the Leginon database infrastructure. The contrast transfer function for each micrograph was automatically estimated and applied to the micrographs before particle extraction. A total of 30,677 particles were automatically selected from the micrographs and were subsequently assessed manually for accuracy. Mature particles were extracted at a box size of 1,280 pixels and binned by a factor of 2 for processing. The final stack contained 20,983 particles. We carried out the 3D reconstruction using the EMAN reconstruction package (Ludtke et al., 1999) followed by eight iterations of refinement with the Frealign package (Grigorieff, 2007). Resolution was assessed by calculating the Fourier shell correlation at a cutoff of 0.5, which provided a value of 8.5 Å resolution.

Prohead particles were observed alongside mature particles in the two cryoEM data sets, and 1,179 particles were manually selected. Particles were preprocessed in the same manner as the mature particles.

ACCESSION NUMBERS

The cryoEM density maps for the mature and immature phage are available at the EM Databank (http://www.emdatabank.org) under accession numbers 5382 and 5383, respectively.

ACKNOWLEDGMENTS

We thank Oleg Stens and Megan Escalona for assistance in purification and preparation of the SIO-2 virus for structural characterization. Xavier Bailly (Station Biologique de Roscoff) aided in bioinformatics analysis of the SIO-2 genome. This project was funded by grants from the National Institutes of Health (NIH) through the National Center for Research Resources P41 Program (Grants RR17573 and RR023093), NIH Grant R01 GM054076 to J.E.J., and a grant from the Gordon and Betty Moore Foundation Marine Microbiology Initiative to F.A., with additional funding to A.-C. B. by a Scripps Institute of Oceanography postdoctoral fellowship and to G.C.L. by an ARCS Foundation fellowship.

Received: August 3, 2011
Revised: December 30, 2011
Accepted: January 10, 2012
Published: March 6, 2012

REFERENCES

Agirrezabala, X., Velázquez-Muriel, J.A., Gómez-Puertas, P., Scheres, S.H., Carazo, J.M., and Carrascosa, J.L. (2007). Quasi-atomic model of bacteriophage t7 procapsid shell: insights into the structure and evolution of a basic fold. Structure *15*, 461–472.

Baker, M.L., Jiang, W., Rixon, F.J., and Chiu, W. (2005). Common ancestry of herpesviruses and tailed DNA bacteriophages. J. Virol. *79*, 14967–14970.

Bamford, D.H., Grimes, J.M., and Stuart, D.I. (2005). What does structure tell us about virus evolution? Curr. Opin. Struct. Biol. *15*, 655–663.

Baudoux, A.C., Hendrix, R.W., Lander, G.C., Bailly, X., Podell, S., Paillard, C., Johnson, J.E., Potter, C.S., Carragher, B., and Azam, F. (2012). Genomic and functional analysis of Vibrio phage SIO-2 reveals novel insights into ecology and evolution of marine siphoviruses. Environ. Microbiol., in press. Published online January 9, 2012. 10.1111/j.1462-2920.2011.02685.x.

Caspar, D.L., and Klug, A. (1962). Physical principles in the construction of regular viruses. Cold Spring Harb. Symp. Quant. Biol. *27*, 1–24.

Duda, R.L., Hendrix, R.W., Huang, W.M., and Conway, J.F. (2006). Shared architecture of bacteriophage SPO1 and herpesvirus capsids. Curr. Biol. *16*, R11–R13.

Fokine, A., Leiman, P.G., Shneider, M.M., Ahvazi, B., Boeshans, K.M., Steven, A.C., Black, L.W., Mesyanzhinov, V.V., and Rossmann, M.G. (2005). Structural and functional similarities between the capsid proteins of bacteriophages T4 and HK97 point to a common ancestry. Proc. Natl. Acad. Sci. USA *102*, 7163–7168.

Fokine, A., Islam, M.Z., Zhang, Z., Bowman, V.D., Rao, V.B., and Rossmann, M.G. (2011). Structure of the three N-terminal immunoglobulin domains of the highly immunogenic outer capsid protein from a T4-like bacteriophage. J. Virol. *85*, 8141–8148.

Fraser, J.S., Yu, Z., Maxwell, K.L., and Davidson, A.R. (2006). Ig-like domains on bacteriophages: a tale of promiscuity and deceit. J. Mol. Biol. *359*, 496–507.

Freiberg, A.N., Sherman, M.B., Morais, M.C., Holbrook, M.R., and Watowich, S.J. (2008). Three-dimensional organization of Rift Valley fever virus revealed by cryoelectron tomography. J. Virol. *82*, 10341–10348.

Gan, L., Speir, J.A., Conway, J.F., Lander, G., Cheng, N., Firek, B.A., Hendrix, R.W., Duda, R.L., Liljas, L., and Johnson, J.E. (2006). Capsid conformational sampling in HK97 maturation visualized by X-ray crystallography and cryo-EM. Structure *14*, 1655–1665.

Gertsman, I., Gan, L., Guttman, M., Lee, K., Speir, J.A., Duda, R.L., Hendrix, R.W., Komives, E.A., and Johnson, J.E. (2009). An unexpected twist in viral capsid maturation. Nature *458*, 646–650.

Grigorieff, N. (2007). FREALIGN: high-resolution refinement of single particle structures. J. Struct. Biol. *157*, 117–125.

Harauz, G., and Van Heel, M. (1986). Exact filters for general geometry three dimensional reconstruction. Optik (Stuttg.) *73*, 146–156.

 ©2012 Elsevier Ltd All rights reserved

Helgstrand, C., Wikoff, W.R., Duda, R.L., Hendrix, R.W., Johnson, J.E., and Liljas, L. (2003). The refined structure of a protein catenane: the HK97 bacteriophage capsid at 3.44 A resolution. J. Mol. Biol. *334*, 885–899.

Hendrix, R.W. (1999). Evolution: the long evolutionary reach of viruses. Curr. Biol. *9*, R914–R917.

Hendrix, R.W. (2002). Bacteriophages: evolution of the majority. Theor. Popul. Biol. *61*, 471–480.

Huiskonen, J.T., Overby, A.K., Weber, F., and Grünewald, K. (2009). Electron cryo-microscopy and single-particle averaging of Rift Valley fever virus: evidence for GN-GC glycoprotein heterodimers. J. Virol. *83*, 3762–3769.

Jiang, W., Chang, J., Jakana, J., Weigele, P., King, J., and Chiu, W. (2006). Structure of epsilon15 bacteriophage reveals genome organization and DNA packaging/injection apparatus. Nature *439*, 612–616.

Jiang, W., Baker, M.L., Jakana, J., Weigele, P.R., King, J., and Chiu, W. (2008). Backbone structure of the infectious epsilon15 virus capsid revealed by electron cryomicroscopy. Nature *451*, 1130–1134.

Johnson, J.E. (2010). Virus particle maturation: insights into elegantly programmed nanomachines. Curr. Opin. Struct. Biol. *20*, 210–216.

Lander, G.C., Evilevitch, A., Jeembaeva, M., Potter, C.S., Carragher, B., and Johnson, J.E. (2008). Bacteriophage lambda stabilization by auxiliary protein gpD: timing, location, and mechanism of attachment determined by cryo-EM. Structure *16*, 1399–1406.

Lander, G.C., Stagg, S., Voss, N.R., Cheng, A., Fellmann, D., Pulokas, J., Yoshioka, C., Irving, C., Mulder, A., Lau, P., et al. (2009). Appion: an integrated, database-driven pipeline to facilitate EM image processing. J. Struct. Biol. *166*, 95–102.

Lee, K.K., Tsuruta, H., Hendrix, R.W., Duda, R.L., and Johnson, J.E. (2005). Cooperative reorganization of a 420 subunit virus capsid. J. Mol. Biol. *352*, 723–735.

Long, R.A., and Azam, F. (2001). Antagonistic interactions among marine pelagic bacteria. Appl. Environ. Microbiol. *67*, 4975–4983.

Ludtke, S.J., Baldwin, P.R., and Chiu, W. (1999). EMAN: semiautomated software for high-resolution single-particle reconstructions. J. Struct. Biol. *128*, 82–97.

Mannige, R.V., and Brooks, C.L., 3rd. (2010). Periodic table of virus capsids: implications for natural selection and design. PLoS ONE *5*, e9423.

Morais, M.C., Choi, K.H., Koti, J.S., Chipman, P.R., Anderson, D.L., and Rossmann, M.G. (2005). Conservation of the capsid structure in tailed dsDNA bacteriophages: the pseudoatomic structure of phi29. Mol. Cell *18*, 149–159.

Overby, A.K., Pettersson, R.F., Grünewald, K., and Huiskonen, J.T. (2008). Insights into bunyavirus architecture from electron cryotomography of Uukuniemi virus. Proc. Natl. Acad. Sci. USA *105*, 2375–2379.

Parent, K.N., Khayat, R., Tu, L.H., Suhanovsky, M.M., Cortines, J.R., Teschke, C.M., Johnson, J.E., and Baker, T.S. (2010). P22 coat protein structures reveal a novel mechanism for capsid maturation: stability without auxiliary proteins or chemical crosslinks. Structure *18*, 390–401.

Sousa, D., and Grigorieff, N. (2007). Ab initio resolution measurement for single particle structures. J. Struct. Biol. *157*, 201–210.

Suloway, C., Pulokas, J., Fellmann, D., Cheng, A., Guerra, F., Quispe, J., Stagg, S., Potter, C.S., and Carragher, B. (2005). Automated molecular microscopy: the new Leginon system. J. Struct. Biol. *151*, 41–60.

Suttle, C.A. (2007). Marine viruses—major players in the global ecosystem. Nat. Rev. Microbiol. *5*, 801–812.

Wikoff, W.R., Liljas, L., Duda, R.L., Tsuruta, H., Hendrix, R.W., and Johnson, J.E. (2000). Topologically linked protein rings in the bacteriophage HK97 capsid. Science *289*, 2129–2133.

 ©2012 Elsevier Ltd All rights reserved